RESEARCH ARTICLE

CME

Cortical [^{18}F]PI-2620 Binding Differentiates Corticobasal Syndrome Subtypes

Carla Palleis, MD,[1,2†] Matthias Brendel, MD,[3,4†] Anika Finze,[3] Endy Weidinger, MD,[1,2] Kai Bötzel, MD,[1] Adrian Danek, MD,[1] Leonie Beyer, MD,[3] Alexander Nitschmann,[3] Maike Kern,[3] Gloria Biechele,[3] Boris-Stephan Rauchmann, MD,[5,6] Jan Häckert, MD,[6] Matthias Höllerhage, MD,[7] Andrew W. Stephens, MD, PhD,[8] Alexander Drzezga, MD,[9,10,11] Thilo van Eimeren, MD,[9,10,12] Victor L. Villemagne, MD,[13] Andreas Schildan, PhD,[14] Henryk Barthel, MD,[14] Marianne Patt, PhD,[14] Osama Sabri, MD,[14] German Imaging Initiative for Tauopathies (GII4T), Peter Bartenstein, MD,[3,4] Robert Perneczky, MD,[2,4,6,15] Christian Haass, PhD,[2,4,16] Johannes Levin, MD,[1,2,4†*] and Günter U. Höglinger, MD[2,4,7†*]

[1]*Department of Neurology, Ludwig-Maximilians-University, Munich, Germany*
[2]*German Center for Neurodegenerative Diseases (DZNE), Munich, Germany*
[3]*Department of Nuclear Medicine, Ludwig-Maximilians-University, Munich, Germany*
[4]*Munich Cluster for Systems Neurology (SyNergy), Munich, Germany*
[5]*Department of Radiology, Ludwig-Maximilians-University, Munich, Germany*
[6]*Department of Psychiatry and Psychotherapy, Ludwig-Maximilians-University, Munich, Germany*
[7]*Department of Neurology, Hannover Medical School, Hannover, Germany*
[8]*Life Molecular Imaging GmbH, Berlin, Germany*
[9]*Department of Nuclear Medicine, Faculty of Medicine and University Hospital Cologne, University of Cologne, Cologne, Germany*
[10]*German Center for Neurodegenerative Diseases (DZNE), Bonn-Cologne, Germany*
[11]*Institute of Neuroscience and Medicine (INM-2), Molecular Organization of the Brain, Forschungszentrum Jülich, Julich, Germany*
[12]*Department of Neurology, University Hospital Cologne, Cologne, Germany*
[13]*Department of Psychiatry, The University of Pittsburgh, Pittsburgh, Pennsylvania, USA*
[14]*Department of Nuclear Medicine, University of Leipzig, Leipzig, Germany*
[15]*Ageing Epidemiology (AGE) Research Unit, School of Public Health, Imperial College, London, United Kingdom*
[16]*Chair of Metabolic Biochemistry, Biomedical Center (BMC), Faculty of Medicine, Ludwig-Maximilians-University, Munich, Germany*

***Correspondence to:** Dr. J. Levin, Department of Neurology University of Munich and German Center of Neurodegenerative Diseases (DZNE) e.V., Marchioninistraße 15, 81377 Munich, Germany; E-mail: johannes.levin@med.uni-muenchen.de; or Dr. G.U. Höglinger, Department of Neurology, Medizinische Hochschule Hannover; Carl-Neuberg-Str. 1, 30625 Hannover, Germany; E-mail: guenter.hoeglinger@dzne.de

[†]Contributed equally.

Members of the German Imaging Initiative for Tauopathies (GII4T) Study Group are listed in the Appendix.

Relevant conflicts of interest/financial disclosures: M.B. received speaker honoraria from GE Healthcare and LMI and is an adviser of LMI. G.U.H. has ongoing research collaborations with Prothena; serves as a consultant for AbbVie, AlzProtect, Asceneuron, Biogen, Biohaven, Lundbeck, Novartis, Roche, Sanofi, UCB; received honoraria for scientific presentations from AbbVie, Bial, Biogen, Bristol Myers Squibb, Roche, Teva, UCB, and Zambon; and holds a patent on PERK Activation for the Treatment of Neurodegenerative Diseases (PCT/EP2015/068734). C.H. is chief scientific adviser of ISAR Biosciences and collaborates with DENALI Therapeutics. R.P. is on the advisory board for Biogen, has consulted for Eli Lilly, is a grant recipient from Janssen Pharmaceutica and Boehringer Ingelheim, and has received speaker honoraria from Janssen-Cilag, Pfizer, and Biogen. J.L. reports speaker fees from Bayer Vital, consulting fees from Axon Neuroscience, author fees from Thieme medical publishers and W. Kohlhammer GmbH medical publishers, nonfinancial support from AbbVie and compensation for duty as part-time CMO from MODAG GmbH, all outside the submitted work. O.S. receives research funding from LMI. A.W.S. is an employee of LMI. All other authors report no conflicts of interest.

Funding agencies: This work was funded by the Deutsche Forschungsgemeinschaft (DFG, German Research Foundation) to P.B. and N.A. — project number 421887978, to C.W. — project number DFG WE2298/10-1, 422182557, and to A.R. and M.B. — project numbers BR4580/1-1/ RO5194/1-1. The recruitment of the ActiGliA cohort was supported by the presidential fund of the Helmholtz Society (to C.H.). This project was also supported by the German Center for Neurodegenerative Diseases (DZNE, DescribePSP Study), the German Parkinson's Association (DPG, ProPSP Study), and the Hirnliga e.V. (Manfred-Strohscheer-Stiftung). Tau PET imaging was funded by the Alzheimer Forschung Initiative e.V. (grant 19063p). C.P., P.B., G.U.H., C.H., J.L., and R.P. were supported by the Deutsche Forschungsgemeinschaft (DFG, German Research Foundation) under Germany's Excellence Strategy within the framework of the Munich Cluster for Systems Neurology (EXC 2145 SyNergy – ID 390857198). G.U.H. and C.H. were also funded by the NOMIS Foundation (FTLD project), Volkswagen Stiftung/Lower Saxony Ministry for Science/ Petermax-Müller Foundation (Etiology and Therapy of Synucleinopathies and Tauopathies). The Lüneburg Heritage has supported the work of C.P. and J.L. L.B. was funded by the Munich-Clinician-Scientist Program.

Received: 30 January 2021; **Revised:** 23 March 2021; **Accepted:** 5 April 2021

Published online 5 May 2021 in Wiley Online Library (wileyonlinelibrary.com). DOI: 10.1002/mds.28624

ABSTRACT: Background: Corticobasal syndrome is associated with cerebral protein aggregates composed of 4-repeat (~50% of cases) or mixed 3-repeat/4-repeat tau isoforms (~25% of cases) or nontauopathies (~25% of cases).

Objectives: The aim of this single-center study was to investigate the diagnostic value of the tau PET-ligand [18F]PI-2620 in patients with corticobasal syndrome.

Methods: Forty-five patients (71.5 ± 7.6 years) with corticobasal syndrome and 14 age-matched healthy controls underwent [18F]PI-2620-PET. Beta-amyloid status was determined by cerebral β-amyloid PET and/or CSF analysis. Subcortical and cortical [18F]PI-2620 binding was quantitatively and visually compared between β-amyloid-positive and -negative patients and controls. Regional [18F]PI-2620 binding was correlated with clinical and demographic data.

Results: Twenty-four percent (11 of 45) were β-amyloid-positive. Significantly elevated [18F]PI-2620 distribution volume ratios were observed in both β-amyloid-positive and β-amyloid-negative patients versus controls in the dorsolateral prefrontal cortex and basal ganglia. Cortical [18F]PI-2620 PET positivity was distinctly higher in β-amyloid-positive compared with β-amyloid-negative patients with pronounced involvement of the dorsolateral prefrontal cortex. Semiquantitative analysis of [18F]PI-2620 PET revealed a sensitivity of 91% for β-amyloid-positive and of 65% for β-amyloid-negative cases, which is in excellent agreement with prior clinicopathological data. Regardless of β-amyloid status, hemispheric lateralization of [18F]PI-2620 signal reflected contralateral predominance of clinical disease severity.

Conclusions: Our data indicate a value of [18F]PI-2620 for evaluating corticobasal syndrome, providing quantitatively and regionally distinct signals in β-amyloid-positive as well as β-amyloid-negative corticobasal syndrome. In corticobasal syndrome, [18F]PI-2620 may potentially serve for a differential diagnosis and for monitoring disease progression. © 2021 The Authors. *Movement Disorders* published by Wiley Periodicals LLC on behalf of International Parkinson and Movement Disorder Society

Key Words: tau; PET; corticobasal syndrome; four-repeat tauopathies; Alzheimer's disease

Corticobasal syndrome (CBS) is a rare adult-onset disorder characterized by a combination of cortical signs and movement disorder signs. Clinically, CBS can be diagnosed using the Movement Disorder Society (MDS) criteria for progressive supranuclear palsy (PSP)[1] or the corticobasal degeneration (CBD) criteria.[2] The pathology of CBS is characterized by 4-repeat (4R) tau aggregation in CBD and PSP (approximately 50% of patients) or by mixed 3-repeat/4-repeat (3R/4R) tau aggregation in Alzheimer's disease (AD) pathology (about 25%).[1-4] The 4R tauopathies are characterized by intracellular aggregates of tau isoforms with 4 repeats in the microtubule-binding domain in neurons, astrocytes, and oligodendrocytes. There are proposals to classify CBD and PSP as closely related variants within a coherent disease spectrum, that is, 4R tauopathies.[1,5] In rare cases, CBS with rapid decline and early death after diagnosis can occur in prion disease[6] or *C9orf72* mutation carriers.[7] Antemortem misdiagnosis of CBS and the underlying pathologies is very common[8,9] because of a lack of reliable biomarkers and overlapping phenotypes of the different neuropathologies.[4,10] Diagnostic biomarkers are only available for CBS with underlying AD pathology, including β-amyloid (Aβ) PET and quantification of Aβ, total, and phosphorylated tau concentrations in cerebrospinal fluid (CSF).[11-13] The definite diagnosis of the different neuropathological entities underlying CBS relies on postmortem examination. The precise antemortem diagnosis of the molecular pathologies in individual CBS patients, however, becomes more important, as molecularly targeted therapies for the underlying proteinopathies are being developed.[4,10]

Multiple radioligands for PET are currently investigated for their potential to detect tau deposits in vivo. In the first generation of tau-targeting tracers, off-target binding, for example, to monoamine-oxidase B,[14,15] limited the specific visualization of tau burden in vivo.[16-19] The newer tau PET ligand [18F]PI-2620[20] showed less off-target binding to monoamine oxidases, high affinity to 3R/4R tau in AD and recently also revealed binding in the 4R tauopathy PSP.[21]

Therefore, we investigated the utility of [18F]PI-2620 as an in vivo biomarker for CBS and its heterogeneous underlying molecular entities.

Material and Methods

Participants and Clinical Evaluation

The study cohort is embedded in Activity of Cerebral Networks, Amyloid and Microglia in Aging and Alzheimer's Disease (ActiGliA), a prospective cohort study at Ludwig-Maximilians-University (LMU), approved by the local ethics committee (project number 17-755; see File S1 for details; human PET analyses project numbers 17-569 and 19-022). Written informed consent was obtained from all participants in accordance with the Declaration of Helsinki.

Clinical diagnosis of CBS was made as defined in the MDS-PSP criteria.[1] All enrolled patients also fulfilled the Armstrong criteria of probable or possible CBD-CBS.[2] Only patients with negative family history for Parkinson's disease and AD were included.

Disease duration was defined as the time between symptom onset and clinical assessment. For clinical rating, we used the PSP rating scale (PSPRS)[22] and the PSP clinical deficits scale (PSP-CDS).[23] Functional independence was measured using the Schwab and England Activities of Daily Living (SEADL) scale.[24] Cognitive state was assessed with the Montreal Cognitive Assessment (MoCA) scale.[25] The Dementia Apraxia Test (DATE)[26] was used for assessment of buccofacial and upper limb apraxia. Verbal fluency was tested using the lexical fluency task from the Frontal Assessment Battery.[27]

Aβ concentration and Aβ ratio in CSF and [^{18}F] flutemetamol PET served for assessment of the Aβ status (see Methods section, below). In healthy controls, [^{18}F]florbetaben PET within 12 months prior to study inclusion was also accepted. In case of β-amyloid positivity in CSF or PET, patients were classified as CBS with underlying AD pathology (Aβ-positive CBS; Aβ[+] CBS).[12] In case of β-amyloid negativity (Aβ-negative CBS; Aβ[−]CBS), patients were subclassified as CBS with either "suggestive" or "probable" underlying 4R tauopathy.[28,29]

The [^{18}F]PI-2620 PET was performed in 45 CBS patients (see Methods section, below). Distribution of [^{18}F]PI-2620 tracer binding of 8 patients included in the current report has already been reported previously.[21]

Results were compared with 14 age-matched cognitively healthy individuals without motor or cognitive signs or symptoms (CTRL). Four were scanned in Munich, and 10 were scanned in New Haven or Melbourne.[21] There were no statistically significant differences in binding characteristics of [^{18}F]PI-2620 between external and inhouse controls (Table S1 in File S1).

The regional [^{18}F]PI-2620 distribution of Aβ(+)CBS and Aβ(−)CBS patients in the central region for pattern analysis was compared with 12 patients with typical AD dementia or mild cognitive impairment (MCI) according to the diagnostic criteria of the National Institute on Aging and Alzheimer's Association[12] from the ActiGliA cohort. The AD cohort has partially been published previously.[21]

PET Imaging

Tau-PET Acquisition and Analysis

The [^{18}F]PI-2620 acquisition, reconstruction, and harmonization across scanners at the Department of Nuclear Medicine at LMU were performed as described previously[21] (see File S1 for details). The subcortical target regions (putamen, globus pallidus externus, globus pallidus internus, subthalamic nucleus, substantia nigra, dentate nucleus, midbrain), the dorsolateral prefrontal cortex (DLPFC), and the medial prefrontal cortex were identical to the earlier analysis in PSP. Motor cortex, temporal mesial, temporal lateral, parietal, anterior cingulate gyrus, and postcentral cortical target regions of the Hammers atlas[30] were introduced as additional target regions. The maximum distribution volume ratio (DVR) of bilateral regions was used for group comparisons with account for asymmetric tracer distribution in CBS. All images of clinically left-dominant CBS patients were flipped for image visualization. Voxels with a DVR ≥ mean value (MV) + 2 standard deviations (SDs) of the controls were defined as positive and the percentage of positivity was calculated in Aβ(+)CBS, Aβ(−)CBS, and typical AD. The comparison was performed qualitatively. To address potential differences in tracer affinity to 4R- and 3R/4R tau,[20] we generated binarized voxel-based maps of [^{18}F]PI-2620 positivity for all patients and compared the percentage of voxel positivity between Aβ(+)CBS and Aβ(−)CBS. The 12 Aβ-positive patients with typical AD were processed the same way and compared with CBS patients.

Assessment of Aβ Status

[^{18}F]Flutemetamol, or [^{18}F]Florbetaben, PET in some controls, was primarily used to detect Aβ deposition, indicating underlying AD pathophysiology. Eighty-four percent of CBS patients (38 of 45) and 100% of control subjects underwent Aβ-PET imaging as described previously[31,32] (see details in theFile S1). CSF Aβ was assessed in 87% of patients (39 of 45) and in all patients without Aβ-PET. Threshold for Aβ ratio (Aβ [1–42]/Aβ [1–40]) was set to <5.5% according to standardized laboratory diagnostics at LMU.

Statistical Analyses

SPSS (V25; IBM, Ehningen, Germany) was used for statistical testing. Statistical significance was set at $P < 0.05$. Age, PSPRS, PSP-CDS, DATE, SEADL, verbal fluency test, disease duration, and MoCA were compared between the different study groups (Aβ[+]CBS, Aβ[−]CBS, controls) by a 1-way analysis of variance, whereas sex was subject to a chi-square test. [^{18}F]PI-2620 DVRs of predefined target regions (maximum value of bilateral regions) were compared between the study groups by multivariate analysis of variance including age and sex as covariates as well as false discovery rate correction[33] for multiple brain regions. A region-based classification was performed by a semi-quantitative analysis, defining regional DV R ≥ MV + 2 SD of the controls as positive. One positive target

region classified the subject as positive (dichotomous) for the [18F]PI-2620 scan.

Partial correlations (Pearson's coefficient of correlation [R]) were calculated for [18F]PI-2620 DVR in predefined regions (maximum value of bilateral regions) with PSPRS, PSP-CDS, SEADL, DATE, disease duration, verbal fluency test, and MoCA, controlled for age and sex. The analysis was performed separately for Aβ(+)CBS and Aβ(−)CBS.

Asymmetry of [18F]PI-2620 PET scans was judged visually and semiquantitatively. An expert reader rated the presence of asymmetric tracer distribution of the whole scan taking cortical and subcortical regions into account (none, left, right). The asymmetry index for [18F]PI-2620-binding asymmetry was calculated using a subcortical volume of interest composed of the putamen and the globus pallidus because the topology of asymmetry in cortical regions was too heterogeneous for a standardized quantification. Clinical symptoms were graded for asymmetry as 0 (both sides equally affected), 1 (mild clinical asymmetry), 2 (moderate clinical asymmetry), or 3 (strong clinical asymmetry) for left and right hemispheres based on a movement disorder specialist's neurological examination and clinical score findings in the PSPRS and DATE. Agreement of visual [18F]PI-2620-PET asymmetry and the presence of contralateral clinical symptom asymmetry (≥1, asymmetric) was assessed by Fleiss-Kappa. For semiquantitative analysis, Spearman's coefficient of correlation (r_s) was calculated between the asymmetry index of [18F]PI-2620 PET and clinical asymmetry.

Results

Demographics and Amyloid Status

Performance of [18F]PI-2620 PET occurred in 45 patients (71.5 ± 7.6 years) and 14 age-matched controls without clinical evidence of neurodegenerative diseases (67.4 ± 9.5 years). Detailed demographic and clinical data of the study sample are provided in Table 1. Single patient data are provided in File S1 (Table S2 in File S1).

As positive controls for the Aβ PET and CSF analyses, we used data from 12 patients with typical AD (8 women, 4 men; 67.0 ± 8.1 years; 6 with dementia, 6 with MCI), reported in detail elsewhere.[21] In all AD cases, the Aβ status was positive in both CSF and PET.

In the sample of the current study, all 14 controls were amyloid negative (Aβ[−]) in Aβ PET. In all 34 CBS patients with both Aβ PET and CSF available, the Aβ status was consistent for both biomarkers (8 Aβ[+]/26 Aβ[−]).

Twenty-four percent of the CBS cohort (11 of 45) were amyloid positive, indicating AD pathology with atypical, nonamnestic clinical manifestations. Seventy-

TABLE 1 *Demographics at group level*

Demographics	All CBS	Aβ(+) CBS	Aβ(−) CBS	CTRL
n	45	11	34	14
Sex	18 ♂/27 ♀	3 ♂/8 ♀	15 ♂/19 ♀	5 ♂/9 ♀
Age at examination (y)	71.5 ± 7.6	76.2 ± 4.6[b,c]	69.9 ± 7.7[c]	67.4 ± 9.5
Age at disease onset (y)	68.7 ± 7.7	73.5 ± 4.6[c]	67.1 ± 7.9 [c]	n.a.
Disease duration (mo)	32.7 ± 19.7	32.0 ± 20.1	32.8 ± 19.3	n.a.
PSPRS	25.7 ± 12.0	23.3 ± 5.6	26.5 ± 13.3	n.a.
PSP-CDS	2.1 ± 1.0	2.2 ± 1.0	1.9 ± 0.6	n.a.
SEADL	64.8 ± 17.8	66.7 ± 8.2	64.2 ± 19.8	n.a.
Verbal fluency test	1.7 ± 1.1	1.4 ± 1.1	1.8 ± 1.1	n.a.
MoCA	21.3 ± 6.1	16.9 ± 7.3[b,c]	22.6 ± 5.2[a,c]	28.8 ± 1.6
DATE	41.3 ± 13.2	32.6 ± 12.6[c]	43.9 ± 12.4[c]	n.a.
Aβ-positive PET ([18F]flutemetamol or [18F] florbetaben)	9/38	9/9	0/29	0/14
Aβ-positive CSF (Aβ ratio < 5.5%)	10/41	10/10	0/31	0/4
Diagnostic allocation		11 atypical AD with CBS	17 probable CBD-CBS, 17 possible CBD-CBS[2], 24 probable 4R tauopathy, 10 s.o. PSP-CBS[1]	n.a.

Data are presented as mean ± standard deviation, unless indicated otherwise. Demographics were statistically tested by ANOVA or chi-square test.
[a]$P < 0.05$; [b]$P < 0.01$ of group differences between study population and controls; [c]$P < 0.05$ of group differences between Aβ-positive and Aβ-negative CBS patients.

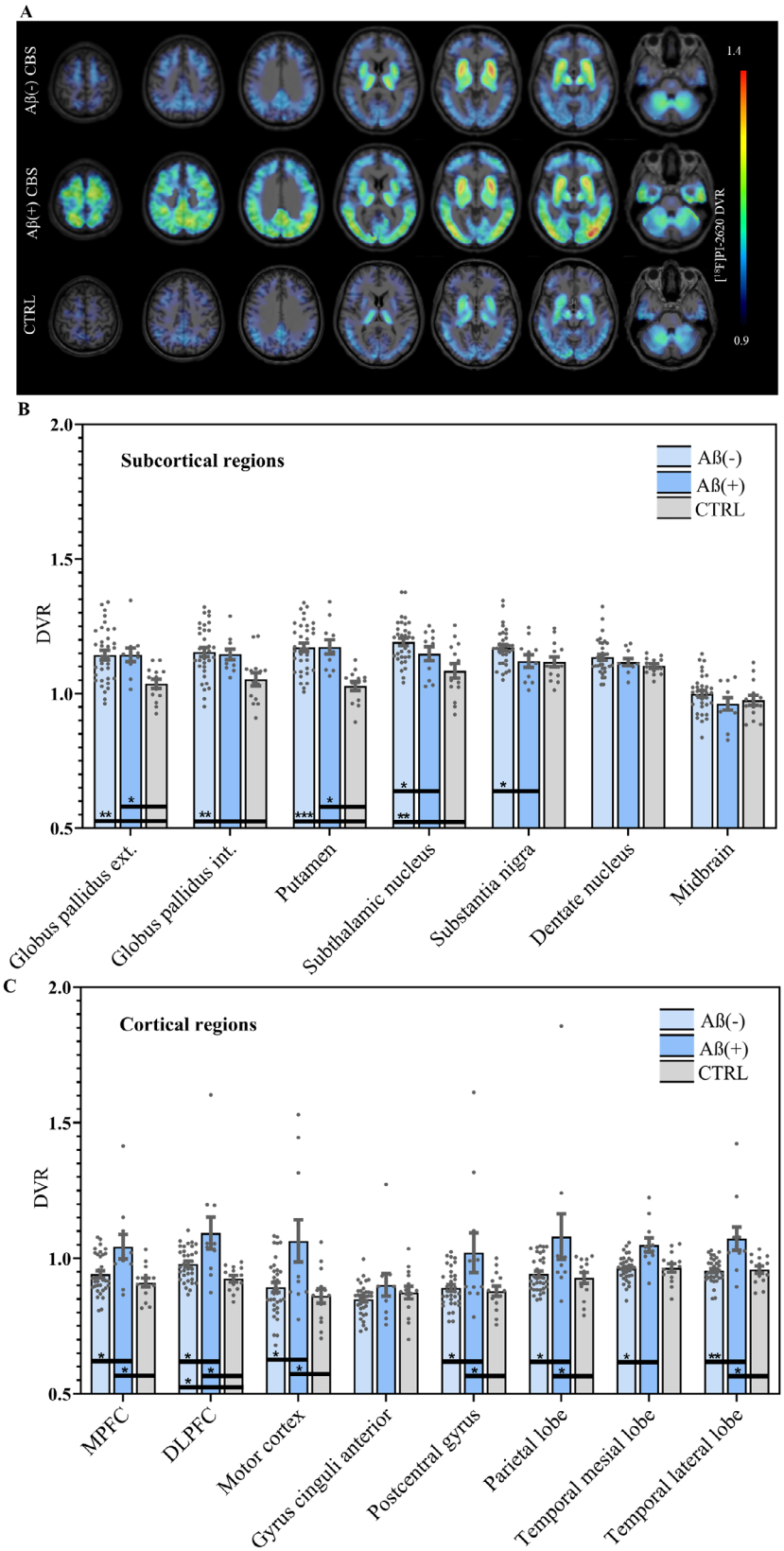

FIG. 1. Voxel-based differences in [^{18}F]PI-2620 binding in predefined tauopathy target regions. (**A**) Average [^{18}F]PI-2620 distribution volume ratio (DVR) binding maps presented as axial overlays on a standard MRI template for all study groups (Aβ[+]CBS, n = 11; Aβ[−]CBS, n = 34; and controls (CTRL), n = 14). Extracerebral voxels were masked. Images from patients with left-dominant symptoms were flipped. (**B**, **C**) [^{18}F]PI-2620 DVR comparison between Aβ(+) CBS, Aβ(−) CBS, and CTRL for 14 evaluated subcortical (**B**) and cortical (**C**) target regions. Statistics derive from multivariate analysis of variance including age and sex as covariates and false discovery rate correction for multiple brain regions. Error bars indicate standard error. *$P < 0.05$; **$P < 0.01$; ***$P < 0.001$ indicate significant [^{18}F]PI-2620-DVR group differences of Aβ(+)CBS and Aβ(−)CBS versus CTRL. [Color figure can be viewed at wileyonlinelibrary.com]

six percent (34 of 45) were amyloid negative (Aβ[−] CBS), of which 10 qualified for "suggestive of PSP with CBS phenotype" and 24 for "probable 4R tauopathy"[1]; 17 cases each fulfilled the diagnosis of CBS with "possible CBD" or "probable CBD," respectively.[2]

Age at examination of Aβ(+)CBS patients (76.2 ± 4.6 years) was significantly higher compared with both Aβ(−)CBS (69.9 ± 7.7 years, $P = 0.0156$) and controls (67.4 ± 9.5 years, $P = 0.0097$). The 2 groups did not significantly differ with regard to disease duration/severity, activities of daily living, and verbal fluency (Table 1).

MoCA was significantly reduced versus controls (28.8 ± 1.6) in both Aβ(+)CBS (16.9 ± 7.3, $P = 0.004$)

TABLE 2 *[18F]PI-2620-PET results at group level*

[18F]PI-2620 distribution volume ratio				Cohen's *d*	
Subcortical target regions	**Aβ(−)CBS, n = 34**	**Aβ(+)CBS, n = 11**	**CTRL, n = 14**	**Aβ(−) CBS/ CTRL**	**Aβ(+) CBS/ CTRL**
Globus pallidus externus	1.143 ± 0.104 (1.107–1.179)[b]	1.144 ± 0.083 (1.088–1.200)[a]	1.037 ± 0.063 (1.000–1.073)	1.242	1.453
Globus pallidus internus	1.154 ± 0.098 (1.120–1.189)[b]	1.146 ± 0.065 (1.102–1.189)	1.053 ± 0.089 (1.002–1.105)	1.082	1.190
Putamen	1.171 ± 0.094 (1.139–1.204)[c]	1.174 ± 0.088 (1.115–1.232)[a]	1.028 ± 0.061 (0.992–1.063)	1.813	1.926
Subthalamic nucleus	1.192 ± 0.079 (1.165–1.220)[b]	1.148 ± 0.085 (1.091–1.205)	1.085 ± 0.103 (1.025–1.144)	1.173	0.672
Substantia nigra	1.171 ± 0.067 (1.147–1.194)	1.121 ± 0.077 (1.069–1.172)	1.118 ± 0.070 (1.077–1.158)	0.769	0.037
Dentate nucleus	1.135 ± 0.065 (1.112–1.158)	1.117 ± 0.043 (1.088–1.146)	1.103 ± 0.031 (1.085–1.121)	0.630	0.385
Midbrain	0.999 ± 0.070 (0.975–1.024)	0.962 ± 0.078 (0.909–1.014)	0.975 ± 0.071 (0.935–1.016)	0.337	−0.184
Cortical target regions	**Aβ(−)CBS, n = 34**	**Aβ(+)CBS, n = 11**	**CTRL, n = 14**	**Aβ(−) CBS/ CTRL**	**Aβ(+) CBS/ CTRL**
MPFC	0.942 ± 0.073 (0.916–0.967)	1.043 ± 0.149 (0.943–1.143)[a]	0.910 ± 0.062 (0.874–0.947)	0.455	1.156
DLPFC	0.979 ± 0.061 (0.957–1.000)[a]	1.093 ± 0.195 (0.962–1.224)[a]	0.925 ± 0.045 (0.899–0.951)	1.000	1.186
Motor cortex	0.893 ± 0.105 (0.856–0.930)	1.064 ± 0.257 (0.891–1.237)[a]	0.861 ± 0.099 (0.804–0.919)	0.307	1.040
Anterior cingulate gyrus	0.849 ± 0.059 (0.828–0.870)	0.902 ± 0.138 (0.809–0.995)	0.874 ± 0.088 (0.823–0.925)	−0.332	0.243
Postcentral gyrus	0.891 ± 0.071 (0.866–0.916)	1.021 ± 0.244 (0.857–1.184)[a]	0.879 ± 0.071 (0.838–0.920)	0.173	0.788
Parietal lobe	0.942 ± 0.065 (0.919–0.965)	1.080 ± 0.277 (0.894–1.266)[a]	0.928 ± 0.073 (0.885–0.970)	0.207	0.753
Temporal mesial lobe	0.963 ± 0.047 (0.946–0.979)	1.049 ± 0.087 (0.991–1.107)	0.965 ± 0.057 (0.932–0.998)	−0.039	1.147
Temporal lateral lobe	0.955 ± 0.045 (0.939–0.970)	1.073 ± 0.142 (0.977–1.168)[a]	0.958 ± 0.051 (0.929–0.988)	−0.079	1.072

Values represent regional group means of [18F]PI-2620 distribution volume ratios as determined by PET imaging, the standard error, and their 95% confidence interval in predefined subcortical and cortical brain areas and the effect size Cohen's *d*. Single subject values are illustrated in Figure 1. Significance levels are indicated by [a]$P < 0.05$, [b]$P < 0.01$, [c]$P < 0.001$. *P* values were derived from multivariate analysis of variance with age and sex as covariates and false discovery rate correction for multiple brain regions.

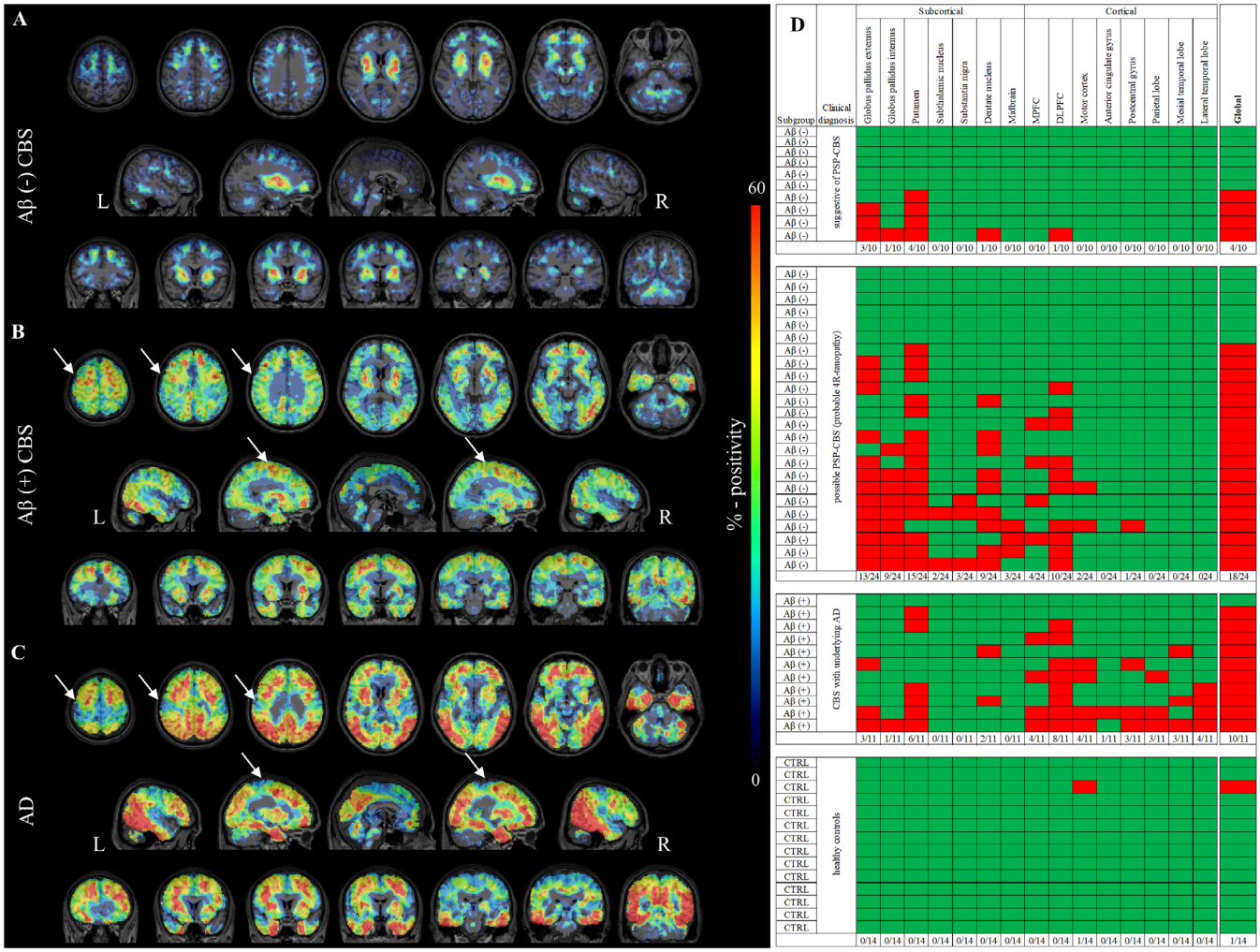

FIG. 2. Regional [^{18}F]PI-2620 PET positivity. (**A**) Aβ(−)CBS, n = 34; (**B**) Aβ(+)CBS, n = 11; (**C**) typical AD, n = 12. (**A–C**) [^{18}F]PI-2620 PET percentage positivity of single voxels was calculated in a 2-step approach. First, binarized maps of [^{18}F]PI-2620 PET positivity were calculated for each patient against controls (MV + 2 SD control threshold). Second, the percentage positivity within the groups of Aβ(+)CBS, Aβ(−)CBS, and Aβ(+)-typical AD was calculated and illustrated. Arrows highlight the pre- and postcentral gyri that are spared from tracer deposition in Aβ(+) typical AD but rich in tracer deposition in Aβ(+)CBS. (**D**) For a multiregion classifier for diagnosis of CBS by [^{18}F]PI-2620 PET, semiquantitative classification (red, positive; green, negative) of CBS target regions was performed by applying a threshold of mean + 2 standard deviations as obtained from the controls without objectified memory impairment and with intact motor function. One positive region defined the scan as global positive (Global). Aβ(−)CBS patients are arranged according to the MDS-PSP criteria.[1] [Color figure can be viewed at wileyonlinelibrary.com]

and Aβ(−)CBS (22.6 ± 5.2, $P = 0.0124$), with Aβ(+) CBS patients significantly more affected by cognitive impairment than Aβ(−)CBS patients ($P = 0.0126$).

The DATE yielded significantly lower scores (indicating more prominent apraxia) in Aβ(+)CBS patients (32.6 ± 12.6) compared with Aβ(−)CBS patients (43.9 ± 12.4, $P = 0.0294$).

Distribution of [^{18}F]PI-2620 Binding

Predefined subcortical regions of interest had significantly elevated [^{18}F]PI-2620 DVRs in both CBS groups versus controls, with the strongest differences in putamen (Fig. 1A,B; Table 2). Aβ(+)CBS displayed higher [^{18}F]PI-2620 DVRs compared with controls in several cortical target regions (Fig. 1A,C; Table 2). Aβ(−)CBS patients showed higher [^{18}F]PI-2620 DVRs compared with controls in the DLPFC (Fig. 1A,C; Table 2).

In both CBS groups, regional subcortical [^{18}F]PI-2620 positivity (threshold > MV + 2 SD of controls) was of similar magnitude (Fig. 2A,B). Aβ(+)CBS patients yielded regional [^{18}F]PI-2620 positivity compared with Aβ(−)CBS in cortical areas, most pronounced in the central region and prefrontal cortex (Fig. 2A,B). Only Aβ(+)CBS patients also showed regional [^{18}F]PI-2620 positivity versus controls in pre- and postcentral gyri, which were spared in Aβ(+) typical AD patients with amnestic syndromes,[21] used as a positive control data set (Fig. 2B,C).

A multiregion classifier for [^{18}F]PI-2620 using a DVR threshold (>MV + 2 SD of controls) was calculated to

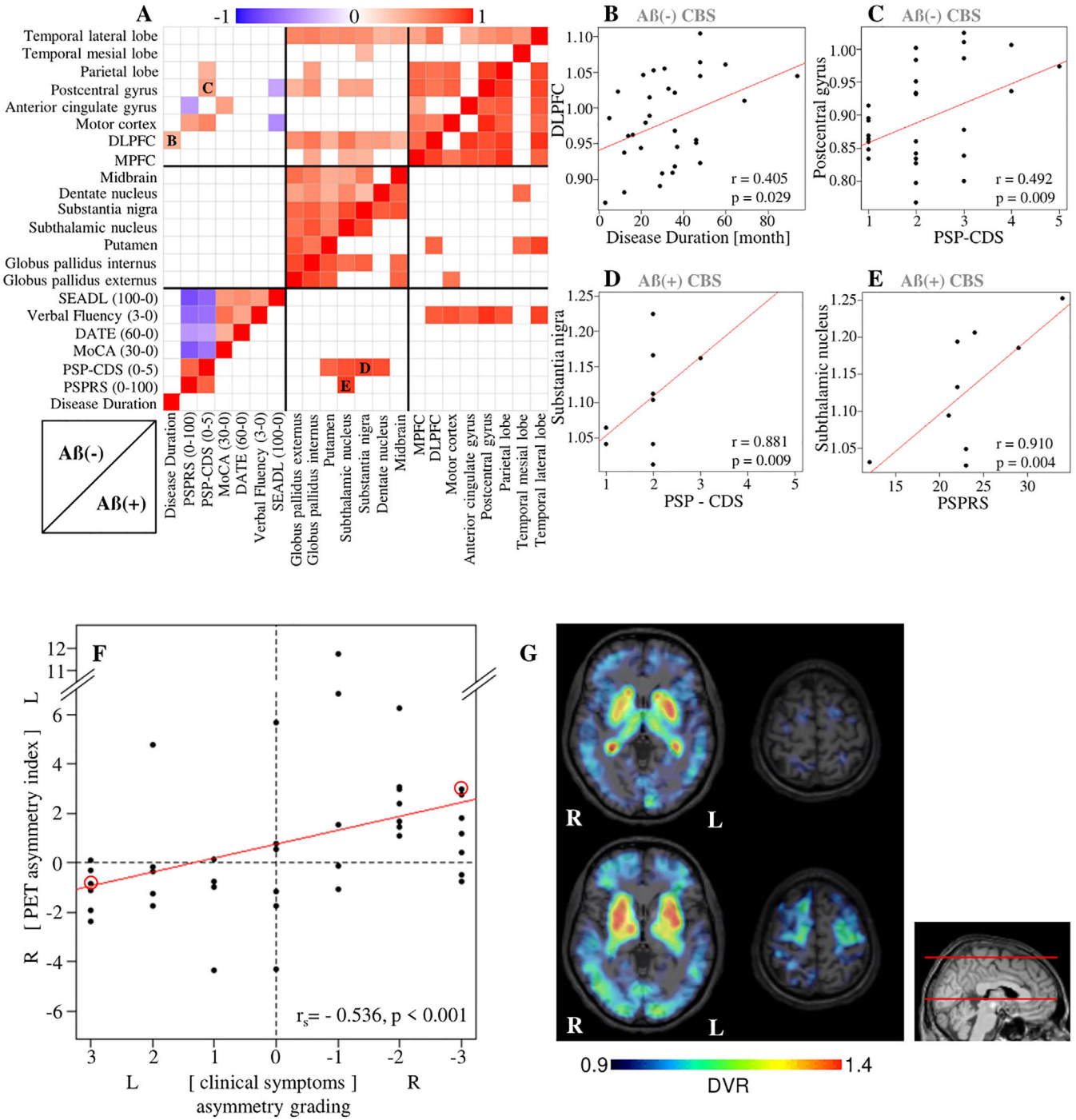

FIG. 3. Correlations between clinical symptoms and [^{18}F]PI-2620 PET in CBS. (**A**) Correlation matrix between [^{18}F]PI-2620 DVR in all evaluated target regions and clinical parameters. Color coding illustrates partial correlations (Pearson's coefficient of correlation, red, positive; purple, negative) with correction for age and sex. The analysis was performed separately for Aβ-positive and Aβ-negative CBS patients. Only associations with a significance of $P < 0.05$ are illustrated. (**B**–**E**) Key associations between parameters of disease duration/progression and [^{18}F]PI-2620-DVR data. R/*P* values derive from partial correlation, controlled for age and sex. (**F**) Asymmetric clinical presentation (asymmetry grading between left- and right-dominant symptoms) as a function of the [^{18}F]PI-2620 PET asymmetry index in n = 41 CBS patients. The degree of association was calculated by Spearman's correlation coefficient. (**G**) Exemplary subcortical [^{18}F]PI-2620-DVR binding in a clinically right-dominant patient (upper row) and a clinically left-dominant patient (lower row). [Color figure can be viewed at wileyonlinelibrary.com]

identify CBS patients based on PET data (Fig. 2D). This approach yielded a sensitivity of 71% for the total cohort (32 of 45), of 91% for Aβ(+)CBS, and of 65% for Aβ(−)CBS.

Cortical [^{18}F]PI-2620 binding in predefined target regions was positive in 47% of all patients (21 of 45), in 82% of Aβ(+)CBS patients (9 of 11), and in 35% of Aβ(−)CBS patients (12 of 34); see Figure 2D. The

DLPFC was the most frequently involved cortical target region compared with controls (Aβ(+)CBS, 73%; Aβ(−)CBS, 32%).

Associations of [^{18}F]PI-2620 Binding With Clinical Symptoms

To assess the potential of [^{18}F]PI-2620 as a biomarker of disease severity, a correlation analysis of [^{18}F]PI-2620 DVR in predefined target regions and clinical parameters was performed.

Figure 3A shows a correlation matrix between all target regions and clinical parameters. In general, clinical scales correlated well with each other in Aβ(−)CBS, but less so in Aβ(+)CBS patients. Also [^{18}F]PI-2620 DVRs in subcortical regions correlated well with each other in Aβ(−)CBS patients, but less so in Aβ(+)CBS patients. Inversely, [^{18}F]PI-2620 DVRs in cortical regions correlated well with each other in Aβ(+)CBS patients, but less so in Aβ(−)CBS patients.

Key associations between [^{18}F]PI-2620-DVR data and clinical parameters corrected for age, sex, and multiple comparisons are displayed in Figure 3B–E.

In Aβ(−)CBS, but not Aβ(+)CBS, disease duration was positively correlated with [^{18}F]PI-2620 DVRs in the DLPFC ($R = 0.405$, $P = 0.029$; Fig. 3A,B). Also, PSP-CDS scores were positively correlated with [^{18}F]PI-2620 DVRs in cortical regions (Fig. 3A), most pronounced in the postcentral gyrus ($R = 0.492$, $P = 0.009$; Fig. 3C) in Aβ(−)CBS, but not Aβ(+) CBS. In Aβ(−)CBS patients, [^{18}F]PI-2620 DVR in subcortical target regions did not correlate significantly with clinical parameters.

In contrast, in Aβ(+)CBS patients, PSP-CDS scores were positively correlated with [^{18}F]PI-2620 DVRs in subcortical regions (Fig. 3A), most pronounced in the substantia nigra ($R = 0.881$, $P = 0.009$; Fig. 3D). Also, PSPRS scores were positively correlated with [^{18}F]PI-2620 DVR in the subthalamic nucleus ($R = 0.910$, $P = 0.004$; Fig. 3A,E) in Aβ(+)CBS, but not Aβ(−)CBS. Verbal fluency positively correlated with [^{18}F]PI-2620 DVR in several cortical areas (Fig. 3A) only in Aβ(+) CBS patients. Tracer binding did not significantly correlate with MoCA, DATE, or SEADL.

With regard to asymmetry of phenotype manifestations, asymmetric presentation of subcortical and cortical symptoms coincided on the same side of the body in all patients (see File S1 for details). An observer-blinded visual read of the asymmetry of [^{18}F]PI-2620 tracer uptake matched the contralateral clinical dominance in 75% of cases (see Table S3 in File S1). A semiquantitative analysis of asymmetry indicated that lateralization of the [^{18}F]PI-2620 signal reflected asymmetry of clinical symptoms in CBS to the hemisphere contralateral of the clinical phenotype ($r_s = -0.536$, $P < 0.001$; Fig. 3F). Figure 3G shows an exemplary subcortical [^{18}F]PI-2620-DVR binding in a clinically left-dominant patient and right-dominant patient.

Discussion

We present the first study applying the novel tau PET tracer [^{18}F]PI-2620 in a cohort of CBS patients with underlying probable 3R/4R- or 4R tauopathy. Our data indicate elevated tracer retention in cortical and subcortical brain areas of Aβ(+)CBS and Aβ(−)CBS patients when compared with cognitively healthy controls without motor symptoms. Strongest binding differences between CBS patients and controls were seen in the putamen and in the globus pallidus. Cortical binding was higher and more frequent in Aβ(+)CBS compared with Aβ(−)CBS patients, with DLPFC being the most frequently positive cortical area in both subgroups. In additional, Aβ(+)CBS patients showed an elevated [^{18}F]PI-2620 binding in pre- and postcentral gyri in contrast to amnestic AD patients. A positive [^{18}F]PI-2620 PET was observed in 91% of Aβ(+)CBS patients and in 65% of all Aβ(−)CBS patients, which is in excellent agreement with prior clinicopathological data. Aβ status in amyloid PET and CSF was coherent in all CBS patients, with Aβ positivity in 24%. Asymmetry of [^{18}F]PI-2620-PET binding corresponded to the contralateral dominance of the clinical phenotype.

The main question still remained: if the next-generation tau-PET ligands have the ability to capture 4R tau in vivo. Subcortical brain areas are subject to several relevant off-target sources such as neuromelanin, iron, or microhemorrhage,[34] but particularly cortical binding in 4R-tauopathy patients could substantiate the claim to image 4R tau in vivo. Our previous [^{18}F]PI-2620 investigation revealed blockable tracer binding in cortical autoradiography of deceased PSP patients, but we were not able to show an elevated cortical signal of PSP patients against controls at the group level by PET in vivo.[21] In the current study, we found a significantly elevated binding in the DLPFC of Aβ(−)CBS patients compared with controls, which was still present after correction for multiple comparisons. Our observation fitted topologically to the cortical predilection sites of CBD, involving the motor cortices, which are also characterized by the strongest neuronal injury.[35] Thus, although we acknowledge missing autopsy validation in CBS patients, our data provide the first promising data suggesting in vivo 4R-tau detection in an Aβ(−)CBS cohort by a next-generation tau tracer with limited off-target binding.[20] As a potential caveat, we note that the tracer binding observed in our study could still derive from a neuropathological process very closely paralleling tau pathology. Claims of 4R-tau binding in vivo indeed need to be interpreted with caution because a quantitative correlation between

[18F]AV-1451 PET and 4R-tau burden in autopsy has been reported[36] despite the low or absent autoradiography binding of this tracer.[34,37] Earlier studies with the 2-arylquinoline [18F]THK5351 suggested to detect tau in CBS in vivo,[38] but the majority of the signal was afterward reported to depend on monoamine oxidase binding.[39] However, a very recent study of [18F]PM-PBB3 also showed tracer binding to 4R tau in vitro and pathology controlled in vivo retention was observed in the motor cortex of few CBS patients.[40] There have been previous studies evaluating [18F]AV-1451 PET in CBS, showing an increase in tracer uptake in the motor cortex and basal ganglia contralateral to the clinical phenotype,[41-43] but these studies investigated substantially smaller CBS cohorts and only 1 study compared 2 Aβ(+)CBS and 6 Aβ(−)CBS with each other.[43]

Together with our study, this suggests that PET imaging of tau pathology is potentially feasible in CBS with fluorinated next-generation tracers with less off-target binding. Barring head-to-head-comparison studies, it is not possible to ascertain which tau-PET tracer performs better than the other.

Importantly, the cortical [18F]PI-2620 signal of Aβ(+) cases was stronger and more widespread compared with that of Aβ(−)CBS cases. This fits to the lower affinity of the compound reported for 4R-tau binding compared with 3R/4R tau,[20] which was also reflected by different kinetic profiles in vivo.[21] Thus, affinity differences need to be taken into account when comparing [18F]PI-2620-PET data quantitatively. To circumvent this issue, we calculated the percentage of patient positivity per voxel in subgroups of Aβ(+)CBS and Aβ(−)CBS, which is less sensitive to differences in the binding magnitude. This approach showed that Aβ(+) and Aβ(−) cases had a similar frequency of [18F]PI-2620 positivity in the basal ganglia but Aβ(+)CBS patients had more frequent [18F]PI-2620-positive voxels in the cortex compared with Aβ(−)CBS patients. The putamen and the external part of the globus pallidus showed the highest discrimination rate in the whole CBS cohort against controls. Noteworthily, our data in PSP with Richardson syndrome patients indicated the best discrimination between patients and controls for the internal part of the globus pallidus and also had more frequent elevation in the subthalamic nucleus and the substantia nigra.[21] Thus, patterns of [18F]PI-2620 binding differed in CBS compared with PSP, indicating a shift in [18F]PI-2620 binding toward brain areas with higher brain function when compared with our clinical PSP series, composed predominantly of Richardson syndrome patients.

Interestingly, cognition was more impaired in Aβ(+) CBS than in Aβ(−)CBS patients, whereas motor symptoms did not differ between the 2 groups. This fits with the high frequency of [18F]PI-2620 positivity in the supplemental motor areas of both groups, whereas parietotemporal areas were only affected in the Aβ(+) CBS group. In addition, we noted a correlation of the [18F]PI-2620 DVRs in cortical regions in Aβ(+)CBS, whereas Aβ(−)CBS [18F]PI-2620 DVRs in subcortical regions correlated with each other.

In contrast to our Aβ(+)CBS cohort, the pre- and postcentral gyri in amnestic AD patients are usually spared of tracer deposition,[21] which may serve as an important diagnostic clue for AD patients with different phenotypes.

Even though [18F]PI-2620 binding was higher in cortical regions in patients with atypical AD with the CBS phenotype, there was no significant correlation between cognition and tracer retention. Relatively low correlations between [18F]PI-2620 binding and the clinical phenotype (cognition, apraxia, verbal fluency) may stem from variable or nonlinear sensitivity of clinical rating scales for the assessment of CBS, especially for Aβ(+) patients. Surprisingly, different CBS-relevant clinical rating scales correlated weakly or not with each other in our cohort of Aβ(+)CBS patients, whereas the same scales correlated well with each other in the Aβ(−)CBS group.

Importantly, we found a positive association between disease duration and [18F]PI-2620 binding in the DLPFC in Aβ(−)CBS, which indicates that neuropathology potentially increases during the disease course in this area. In previous studies, the relation of disease duration or disease severity and early tau-tracer binding has been shown to be inconsistent when 4R tauopathies were assessed.[14,15,44,45] A limitation of the correlation analysis between tracer uptake and disease duration may also be caused by a discrepancy between subjective symptom onset and clinical assessment of cognitive and motor dysfunction, as disease duration is defined as the time between subjective symptom onset and PET imaging. Also, it has to be taken into account that our analysis of comparisons between clinical data and [18F]PI-2620 binding DVRs, was corrected for age and sex, but not for multiple comparisons. Nonetheless, the correlation matrix may already give an impression of potential correlations in larger cohorts.

Longitudinal studies will need to address if an increase over time can be monitored by [18F]PI-2620 PET in CBS.

Amyloid PET and CSF assessments were used to detect the β-amyloid status and were fully matched in all patients, indicating for the first time in CBS patients that both methods serve as a reliable biomarker to predict AD pathology. Either examination may be used for clinical decision taking in CBS patients.

The observed proportion of 24% of the cohort being Aβ positive fits well with the expected distribution of AD neuropathology in CBS[3] and indicates a coherence of postmortem pathology and antemortem biomarker–based classification for Aβ(+)CBS. Proportions of cases

with negative Aβ PET and negative [^{18}F]PI-2620 PET (35%, 12 of 34) are similar to non–4R tauopathy autopsy results of 31% in clinical CBS cases.[3] However, we note a limited sensitivity of the tracer, especially for diagnosis of suggestive of PSP-CBS.

Our more general rating of asymmetry of clinical symptoms corresponded very well with contralateral dominance of [^{18}F]PI-2620 binding, suggesting that neuropathology is detected where it causes brain dysfunction.

Given the nature of a rare disease, the relatively small number of 45 CBS patients, of whom 11 patients were Aβ positive, needs to be considered as a limitation of our study. Furthermore, as all observed patients are still alive, so far there is no autopsy validation available of the studied clinically diagnosed cases. Taken together, longitudinal PET studies and autopsy validation are needed for further exploration of in vivo tau PET as a diagnostic and progression biomarker in CBS.[46] The current Aβ(+) and Aβ(−)CBS study population will be followed clinically and by serial tau PET to address these questions.

Conclusion

Our results show that [^{18}F]PI-2620-PET imaging is a useful biomarker for evaluation of CBS, facilitating detection of heterogeneous neuropathology with differences in tracer binding between probable 3R/4R tauopathy Aβ(+)CBS and Aβ(−)CBS cases. [^{18}F]PI-2620 is a sensitive marker to detect tau binding in Aβ(+)CBS with underlying AD pathology. Elevated cortical tracer binding in the DLPFC was found in both probable 3R/4R and Aβ(−)CBS cases. Hence, [^{18}F]PI-2620 PET may serve as a molecular diagnostic marker, detecting tau pathology in various cortical and subcortical sites. Thus, the combination of [^{18}F]PI-2620 with Aβ status (PET or CSF) in CBS may allow the identification of CBS patients for tau-targeting therapeutic trials.

Future work with autopsy validation and longitudinal imaging and clinical assessment in CBS patients will have to investigate sensitivity to change, that is, the usefulness of [^{18}F]PI-2620 as a progression biomarker and as possible target-engagement marker for therapeutic studies. ■

Acknowledgments: We thank all our patients and their caregivers for making this work possible. Furthermore we thank the cyclotron and radiochemistry crews at DZNE Munich and Leipzig University as well as the PET imaging crew and the Clinical Trials Unit at DZNE Munich. Life Molecular Imaging (LMI) provided material support for the manufacturing of PI-2620 and was involved in the analysis and interpretation of the data. LMI provided financial support to separate studies from which data (5 controls from New Haven and 5 controls from Melbourne) are included in this analysis.

Appendix

German Imaging Initiative for Tauopathies (GII4T)

Sabrina Katzdobler, Catharina Prix, Jonathan Vöglein, Urban Fietzek, Sonja Schönecker, Georg Nübling.

References

1. Hoglinger GU, Respondek G, Stamelou M, et al. Clinical diagnosis of progressive supranuclear palsy: the Movement Disorder Society criteria. Mov Disord 2017;32(6):853–864.
2. Armstrong MJ, Litvan I, Lang AE, et al. Criteria for the diagnosis of corticobasal degeneration. Neurology 2013;80(5):496–503.
3. Ling H, O'sullivan SS, Holton JL, et al. Does corticobasal degeneration exist? A clinicopathological re-evaluation. Brain 2010;133(Pt 7):2045–2057.
4. Rösler TW, Tayaranian Marvian A, Brendel M, et al. Four-repeat tauopathies. Prog Neurobiol 2019;180:101644.
5. Höglinger GU. Is it useful to classify progressive supranuclear palsy and corticobasal degeneration as different disorders? No. Mov Disord Clin Pract 2018;5(2):141–144.
6. Maltête D, Guyant-Maréchal L, Mihout B, Hannequin D. Movement disorders and Creutzfeldt-Jakob disease: a review. Parkinsonism Relat Disord 2006;12(2):65–71.
7. Cali CP, Patino M, Tai YK, et al. C9orf72 intermediate repeats are associated with corticobasal degeneration, increased C9orf72 expression and disruption of autophagy. Acta Neuropathol 2019;138(5):795–811.
8. Litvan I, Agid Y, Goetz C, et al. Accuracy of the clinical diagnosis of corticobasal degeneration: a clinicopathologic study. Neurology 1997;48(1):119–125.
9. Jabbari E, Holland N, Chelban V, et al. Diagnosis across the spectrum of progressive supranuclear palsy and corticobasal syndrome. JAMA Neurol 2019;77(3):377–387.
10. McFarland NR. Diagnostic approach to atypical Parkinsonian syndromes. Continuum (Minneap Minn) 2016;22(4 Movement Disorders):1117–1142.
11. McKhann GM, Knopman DS, Chertkow H, et al. The diagnosis of dementia due to Alzheimer's disease: recommendations from the National Institute on Aging-Alzheimer's Association workgroups on diagnostic guidelines for Alzheimer's disease. Alzheimers Dement 2011;7(3):263–269.
12. Jack CR Jr, Bennett DA, Blennow K, et al. NIA-AA Research Framework: toward a biological definition of Alzheimer's disease. Alzheimers Dement 2018;14(4):535–562.
13. Barthélemy NR, Li Y, Joseph-Mathurin N, et al. A soluble phosphorylated tau signature links tau, amyloid and the evolution of stages of dominantly inherited Alzheimer's disease. Nat Med 2020;26:398–407.
14. Brendel M, Schönecker S, Höglinger G, et al. [(18)F]-THK5351 PET correlates with topology and symptom severity in progressive supranuclear palsy. Front Aging Neurosci 2017;9:440.
15. Schonecker S, Brendel M, Palleis C, et al. PET imaging of astrogliosis and tau facilitates diagnosis of Parkinsonian syndromes. Front Aging Neurosci 2019;11:249.
16. Saint-Aubert L, Lemoine L, Chiotis K, Leuzy A, Rodriguez-Vieitez E, Nordberg A. Tau PET imaging: present and future directions. Mol Neurodegener 2017;12(1):19.
17. Lemoine L, Leuzy A, Chiotis K, Rodriguez-Vieitez E, Nordberg A. Tau positron emission tomography imaging in tauopathies: the added hurdle of off-target binding. Alzheimers Dement (Amst) 2018;10:232–236.
18. Chiotis K, Stenkrona P, Almkvist O, et al. Dual tracer tau PET imaging reveals different molecular targets for (11)C-THK5351 and

(11)C-PBB3 in the Alzheimer brain. Eur J Nucl Med Mol Imaging 2018;45(9):1605–1617.

19. Wren MC, Lashley T, Årstad E, Sander K. Large inter- and intra-case variability of first generation tau PET ligand binding in neurodegenerative dementias. Acta Neuropathol Commun 2018;6(1):34.
20. Kroth H, Oden F, Molette J, et al. Discovery and preclinical characterization of [(18)F]PI-2620, a next-generation tau PET tracer for the assessment of tau pathology in Alzheimer's disease and other tauopathies. Eur J Nucl Med Mol Imaging 2019;46(10):2178–2189.
21. Brendel M, Barthel H, van Eimeren T, et al. Assessment of 18F-PI-2620 as a biomarker in progressive supranuclear palsy. JAMA Neurol 2020;77:1408–1419.
22. Golbe LI, Ohman-Strickland PA. A clinical rating scale for progressive supranuclear palsy. Brain 2007;130(Pt 6):1552–1565.
23. Piot I, Schweyer K, Respondek G, et al. The progressive supranuclear palsy clinical deficits scale. Mov Disord 2020;35(4):650–661.
24. Schwab R, England A. Projection technique for evaluating surgery in Parkinson's disease. In: Gillingham FJ, IML D, eds. Third Symposium on Parkinson's Disease. Edinburgh, UK: E&S Livingston; 1969:152–157.
25. Nasreddine ZS, Phillips NA, Bédirian V, et al. The Montreal Cognitive Assessment, MoCA: a brief screening tool for mild cognitive impairment. J Am Geriatr Soc 2005;53(4):695–699.
26. Johnen A, Frommeyer J, Modes F, Wiendl H, Duning T, Lohmann H. Dementia Apraxia Test (DATE): a brief tool to differentiate behavioral variant frontotemporal dementia from Alzheimer's dementia based on apraxia profiles. J Alzheimers Dis 2016;49(3):593–605.
27. Dubois B, Slachevsky A, Litvan I, Pillon B. The FAB: a Frontal Assessment Battery at bedside. Neurology 2000;55(11):1621–1626.
28. Respondek G, Grimm MJ, Piot I, et al. Validation of the movement disorder society criteria for the diagnosis of 4-repeat tauopathies. Mov Disord 2020;35(1):171–176.
29. Grimm MJ, Respondek G, Stamelou M, et al. Clinical conditions "suggestive of progressive supranuclear palsy"-diagnostic performance. Mov Disord 2020;35:2301–2313.
30. Hammers A, Allom R, Koepp MJ, et al. Three-dimensional maximum probability atlas of the human brain, with particular reference to the temporal lobe. Hum Brain Mapp 2003;19(4):224–247.
31. Brendel M, Schnabel J, Schonecker S, et al. Additive value of amyloid-PET in routine cases of clinical dementia work-up after FDG-PET. Eur J Nucl Med Mol Imaging 2017;44(13):2239–2248.
32. Wollenweber FA, Darr S, Muller C, et al. Prevalence of amyloid positron emission tomographic positivity in poststroke mild cognitive impairment. Stroke 2016;47(10):2645–2648.
33. Benjamini Y, Hochberg Y. Controlling the false discovery rate: a practical and powerful approach to multiple testing. J R Stat Soc B Methodol 1995;57(1):289–300.
34. Aguero C, Dhaynaut M, Normandin MD, et al. Autoradiography validation of novel tau PET tracer [F-18]-MK-6240 on human post-mortem brain tissue. Acta Neuropathol Commun 2019;7(1):37.
35. Beyer L, Meyer-Wilmes J, Schonecker S, et al. Clinical routine FDG-PET imaging of suspected progressive supranuclear palsy and corticobasal degeneration: a gatekeeper for subsequent tau-PET imaging? Front Neurol 2018;9:483.
36. Josephs KA, Whitwell JL, Tacik P, et al. [18F]AV-1451 tau-PET uptake does correlate with quantitatively measured 4R-tau burden in autopsy-confirmed corticobasal degeneration. Acta Neuropathol 2016;132(6):931–933.
37. Lowe VJ, Curran G, Fang P, et al. An autoradiographic evaluation of AV-1451 Tau PET in dementia. Acta Neuropathol Commun 2016;4(1):58.
38. Kikuchi A, Okamura N, Hasegawa T, et al. In vivo visualization of tau deposits in corticobasal syndrome by 18F-THK5351 PET. Neurology 2016;87(22):2309–2316.
39. Ng KP, Pascoal TA, Mathotaarachchi S, et al. Monoamine oxidase B inhibitor, selegiline, reduces (18)F-THK5351 uptake in the human brain. Alzheimers Res Ther 2017;9(1):25.
40. Tagai K, Ono M, Kubota M, et al. High-contrast in-vivo imaging of tau pathologies in Alzheimer's and non-Alzheimer's disease tauopathies. Neuron 2021;109(1):42–58.e8.
41. Niccolini F, Wilson H, Hirschbichler S, et al. Disease-related patterns of in vivo pathology in Corticobasal syndrome. Eur J Nucl Med Mol Imaging 2018;45(13):2413–2425.
42. Tsai RM, Bejanin A, Lesman-Segev O, et al. (18)F-flortaucipir (AV-1451) tau PET in frontotemporal dementia syndromes. Alzheimers Res Ther 2019;11(1):13.
43. Smith R, Schöll M, Widner H, et al. In vivo retention of (18)F-AV-1451 in corticobasal syndrome. Neurology 2017;89(8):845–853.
44. Whitwell JL, Lowe VJ, Tosakulwong N, et al. [(18) F]AV-1451 tau positron emission tomography in progressive supranuclear palsy. Mov Disord 2017;32(1):124–133.
45. Schonhaut DR, McMillan CT, Spina S, et al. (18) F-flortaucipir tau positron emission tomography distinguishes established progressive supranuclear palsy from controls and Parkinson disease: a multicenter study. Ann Neurol 2017;82(4):622–634.
46. van Eimeren T, Antonini A, Berg D, et al. Neuroimaging biomarkers for clinical trials in atypical parkinsonian disorders: Proposal for a Neuroimaging Biomarker Utility System. Alzheimers Dement (Amst) 2019;11:301–309.

Supporting Data

Additional Supporting Information may be found in the online version of this article at the publisher's web-site.